Journal of Power Sources 239 (2013) 315–320

Contents lists available at SciVerse ScienceDirect

Journal of Power Sources

journal homepage: www.elsevier.com/locate/jpowsour

Mechanical and electrochemical performance of composite cathode contact materials for solid oxide fuel cells

Michael C. Tucker [a,*], Lutgard C. DeJonghe [b], Valerie García-Negrón [c], Rosa Trejo [c], Edgar Lara-Curzio [c]

[a] Environmental Energy Technology Division, Lawrence Berkeley National Laboratory, 1 Cyclotron Rd, Berkeley, CA 94720, USA
[b] Materials Sciences Division, Lawrence Berkeley National Laboratory, 1 Cyclotron Rd, Berkeley, CA 94720, USA
[c] Materials Science & Technology Division, Oak Ridge National Laboratory, Oak Ridge, TN 37831-6062, USA

HIGHLIGHTS

- Addition of inorganic binder or glass to SOFC contact materials enhances bonding.
- Added materials do not degrade electrochemical performance.
- 1000 h stable operation achieved.

ARTICLE INFO

Article history:
Received 21 February 2013
Received in revised form
21 March 2013
Accepted 22 March 2013
Available online 2 April 2013

Keywords:
SOFC
Cathode contact material
Adhesion
Mechanical testing

ABSTRACT

The feasibility of adding glass or inorganic binder to conventional SOFC cathode contact materials (CCM) in order to improve bonding to adjacent materials in the cell stack is assessed. Two glasses (SEM-COM SCZ-8 and Schott GM31107) and one inorganic binder (Aremco 644A) are mixed with LSM particles to produce composite CCM pastes. These are used to bond $Mn_{1.5}Co_{1.5}O_4$-coated stainless steel mesh current collectors to anode-supported button cells. The cells are operated at 800 °C for about 1000 h. The cell with SCZ-8 addition to the CCM displays quite stable operation (3.9%/1000 h degradation), whereas the other additives lead to somewhat higher degradation rate. Bonding of the CCM to coated stainless steel coupons is also assessed. Interfacial fracture toughness is determined using a four-point bend test. The fracture toughness for LSM–Schott glass (12.3 N mm^{-1}), LSM–SCZ-8 glass (6.8 N mm^{-1}) and LSM–644A binder (5.4 N mm^{-1}) are significantly improved relative to pure LSM (1.7 N mm^{-1}). Indeed, addition of binder or glass is found to improve bonding of the CCM layer without sacrificing cell performance.

1. Introduction

Assembly of solid oxide fuel cell (SOFC) stacks typically involves mechanically and electrically connecting a number of cells and interconnects in series. Connection of the cathode to the interconnect (or coating on the interconnect) is usually accomplished by compression of the stack using an external load frame, and is often aided by the use of a cathode contact material (CCM). The CCM is an electrically conductive material, and is applied as a paste or ink during stack assembly to form a continuous layer or discrete contact pads. The CCM provides electrical connection between the cathode and interconnect, and can also serve to improve in-plane conduction over the area of the cathode. Fig. 1 indicates placement of the CCM in the fuel cell stack. Often, the CCM is simply a thick layer of the electrocatalyst used in the cathode [1]. For example, a thin LSM–YSZ cathode layer optimized for electrochemical activity can be covered with a thick LSM CCM layer optimized for gas transport and electrical conductivity. A significant limitation of this approach, however, is that most cathode compositions require firing at high temperature (>1100 °C) to achieve good sintering [2]. The use of ferritic stainless steel as the interconnect material limits the firing temperature to 1000 °C or lower. In practice, therefore, using a cathode catalyst CCM in conjunction with a stainless steel interconnect results in low CCM layer strength and minimal adhesion at the CCM/interconnect or CCM/cathode interface.

Our approach to this issue is to fabricate composite mixtures of SOFC cathode material and inorganic binder or glass. Conventional CCM pastes use a cathode material to achieve both bonding and electrical contact. In contrast, the approach we take is to separate

* Corresponding author. Tel.: +1 510 486 5304; fax: +1 510 486 4881.
E-mail address: mctucker@lbl.gov (M.C. Tucker).

0378-7753/$ – see front matter © 2013 Elsevier B.V. All rights reserved.
http://dx.doi.org/10.1016/j.jpowsour.2013.03.130

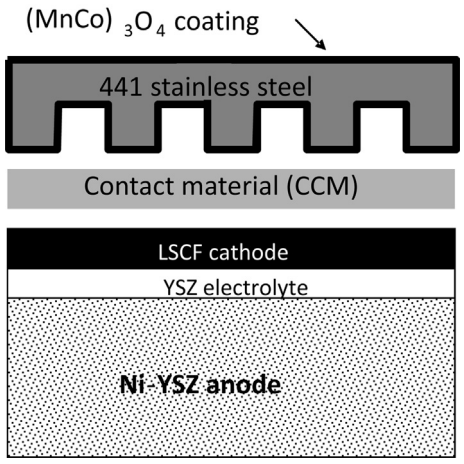

Fig. 1. Schematic representation of CCM placed between SOFC cell and coated stainless steel interconnect.

the functions of electrical contact and mechanical (or chemical) bonding: LSM is the electrical conductor, and the binder or glass serves to improve bonding. In our previous work, we screened a wide variety of glass and binder candidates, and the reader is referred there for a more complete discussion of the candidates and screening methods [3,4]. The most promising composite additives were determined to be Aremco 644A inorganic binder, and SEM-COM SCZ8 and Schott GM31107 glasses. Composites of LSM and these additives were demonstrated to improve bonding to LSCF and $Mn_{1.5}Co_{1.5}O_4$ (MCO)-coated 441 stainless steel at room temperature without sacrificing performance when using a Pt mesh current collector. In this work, we determine mechanical integrity and electrochemical performance under more realistic conditions. Several test methods exist to evaluate the adhesion and fracture toughness of interfaces [5]. In this work we have used a 4-point bend test method initially proposed by Charalambides et al. [6] and further developed by Hofinger et al. [7] because it requires a relatively simple test configuration and specimen geometry. Interfacial fracture toughness of the composites bonded to MCO-coated steel is determined, and electrochemical performance and stability are assessed in the presence of Cr-containing MCO-coated 441 steel current collectors.

2. Experimental methods

2.1. Materials

LSM powder was purchased from Praxair. Glass powders were purchased from SEM-COM (SCZ-8) and Schott (GM31107). Aqueous inorganic binder solution was purchased from Aremco (644A). Pastes were formulated and applied as described elsewhere [3,4]. MCO-coated 441 meshes were prepared by rolling thick 441 coupons (Allegheny Ludlum) down to about 150 μm thick. Perforations were introduced by chemical etching (Italix Company, Inc.), after which both sides were coated with MCO (PNNL), see Fig. 2. Finally, the meshes were flattened and preoxidized by placing between alumina plates and heating to 1000 °C for 1 h.

2.2. Cell testing

Anode supported button cells with LSCF cathode and GDC barrier layer (MSRI) were used. The cathode was coated with CCM paste and an MCO-coated mesh was applied. The glass-containing CCM layers were then sintered at 1000 °C in air for 2 h. The

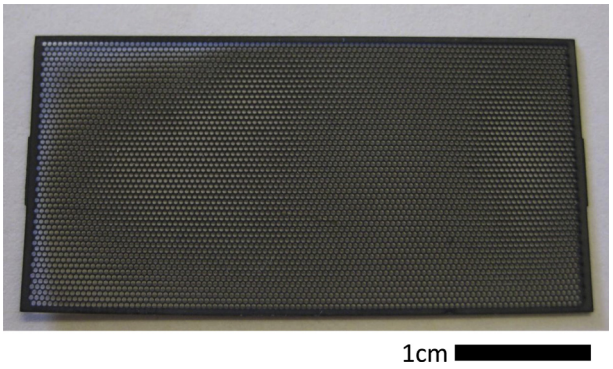

Fig. 2. Photograph of MCO-coated 441 stainless steel mesh prepared by chemical etching.

inorganic binder-containing CCM layer was cured according to the manufacturers' instructions (90° and 360 °C), and heated to 800 °C for 2 h. One cell with Pt mesh attached with Pt paste (Heraeus) to the bare LSCF cathode was prepared as a baseline. The cells were mounted to alumina tubes with Aremco 552 sealant and tested at 800 °C with 97%H_2/3%H_2O fuel and fresh air supplied to the cathode as shown in Fig. 3. The fresh air supply was intended to minimize any interaction between the sealant and Cr-containing mesh, as reported in Ref. [5]. After obtaining initial impedance spectra, the cells were operated at 300 mA cm^{-2} for up to 1000 h. DC current was applied in a 4-probe configuration using a Biologic VMP3 potentiostat.

2.3. SEM

Fracture surfaces of the cells were imaged with SEM and EDS (Hitachi S4300SE/N) after electrochemical operation.

2.4. Mechanical analysis

Specimens for interfacial fracture toughness were prepared from coupons of MCO-coated 441 steel. The coupons were coated with CCM paste and assembled as shown in Fig. 4. The pastes were cured or fired as described above. Dead weight was applied during the heating steps to ensure good contact between the coupons. The specimens were then subjected to 4-point bend testing at the Oak Ridge National Laboratory High Temperature Materials Laboratory using an electromechanical testing machine and a SiC fixture with a support span of 20 mm and a loading span of 10 mm. The diameter

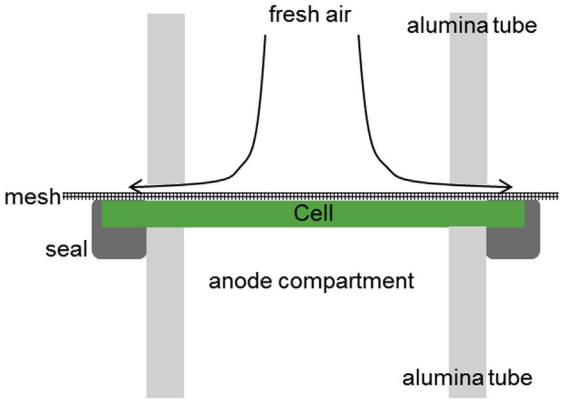

Fig. 3. Schematic of cell testing rig.

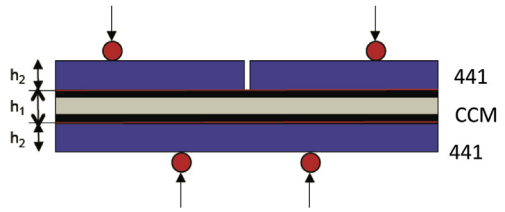

Fig. 4. Mechanical testing specimen geometry.

of the loading pins was 5 mm. The notch was oriented so that it was on the tensile side of the test specimen and the tests were carried out at a constant displacement rate of 5 μm s^{-1}. The formulation presented in Hofinger et al. [7] was followed to calculate the interfacial fracture energy. After testing the tests specimens were examined using scanning electron microscopy to characterize the crack propagation path. Some specimens were further prepared metallographically to obtain precise measurements of the thickness of the different layers in the test specimens.

3. Results and discussion

3.1. Summary of material choice

Previous work focused on proof-of-concept and selection of promising glass and binder candidates for addition to the CCM layer. The most promising binder of those tested was 644A (Aremco), an aqueous solution of aluminum-based inorganic binder, with pH of 4 and no alkaline or alkali earth elements [4]. Upon mixing, the solution coats the LSM particles, and cements them together during drying and curing of the binder. Appropriate binder loading levels were determined such that the mixture was a workable paste, and there was enough binder to enhance bonding yet not so much as to prevent electronic percolation through the layer of LSM particles. Several other binder candidates were eliminated because they reacted with LSM, decreased the conductivity of the CCM layer, or did not improve bonding.

The most promising glass candidates of those tested were SCZ-8 (SEM-COM) and GM31107 (Schott) [3]. Mixtures of glass and LSM were sintered at 1000 °C, and it was found that these glasses resulted in composites that displayed high conductivity, improved hardness, and improved adhesion to other SOFC materials. In contrast, many other glass candidates were eliminated because they reacted with LSM or significantly decreased conductivity of the composite. The softening points for SCZ-8 and Schott are 837 °C and 649 °C, respectively. This large difference in thermal properties leads to dramatically differing microstructures after sintering LSM-glass composites at 1000 °C. For SCZ-8, the composite consisted of glass particles surrounded by an LSM matrix with slightly coarser particles relative to pure LSM. In contrast, the Schott glass particles melt and flow into the surrounding LSM matrix, leaving behind voids where the glass particles were and significantly coarsening and densifying the LSM particles.

3.2. Electrochemical testing

The in-situ test setup employed in this work is intended to reproduce all of the materials interactions and interfaces that might be expected in an operating SOFC stack. We used an MCO-coated 441 stainless steel mesh as the current collector, shown in Fig. 2. This mesh allowed us to include significant CCM/MCO interface area without impeding diffusion of oxygen to the cathode. It also provided a realistic chromium vapor pressure, as the entire mesh was coated with MCO. The MCO deposition technique was not amenable to completely coating the inside of a rib-and-channel interconnect, so we avoided that current collector geometry knowing that the exposed stainless steel surface would introduce a too-high chromium vapor pressure in the vicinity of the cathode that would not be representative of realistic conditions [8].

The initial polarization and AC impedance for cells with MCO-coated 441 mesh current collector bonded with LSM-glass and LSM-binder CCM layers are shown in Fig. 5. Power density in excess of 680 mW cm^{-2} was achieved for LSM–SCZ8 and LSM–644A. The performance for LSM–Schott was slightly lower. Presumably, the maximum power density is higher than this, but larger current densities were not tested so as to avoid overheating of the Pt electrical leads. The observed performance for all composites CCMs was slightly better than similar cells tested with Pt mesh and Pt paste current collector as a baseline (black lines in the figure). AC impedance revealed that the cell with Pt displayed larger ohmic impedance, presumably due to improved current collection in the case of the thicker LSM-based CCM layer and 441 steel mesh.

Fig. 6 shows the stability of the cells operated at 800 °C and 300 mA cm^{-2}. The data for 250 h of operation with Pt mesh and Pt paste are overlaid. The initial cell voltage for LSM–Schott is slightly lower than for Pt, however, this was primarily due to a 26 mV difference in open circuit potential. We therefore do conclude that addition of Schott glass does not lower the cell performance. During the first 600 h of operation, the LSM–Schott cell degraded at a steady rate (20%/1000 h) and then stabilized during the last 400 h. Fig. 7(a) shows AC impedance spectra taken before and after operation. The ohmic impedance increased moderately during operation, presumably due to oxidation of the steel current collecting mesh discussed below. The non-ohmic arc increased significantly, possibly arising from degradation of the LSCF cathode catalyst.

The initial performance and stability for cells with LSM/644A and LSM/SCZ8 are quite good, and nearly identical that of Pt. The electrical conductivity of the LSM/644A and LSM/SCZ8 CCM layers is high enough to not adversely affect cell performance. A stable rate of degradation (3.9%/1000 h) was observed for the cell with LSM/SCZ8 CCM during the entire 1000 h of operation. The addition

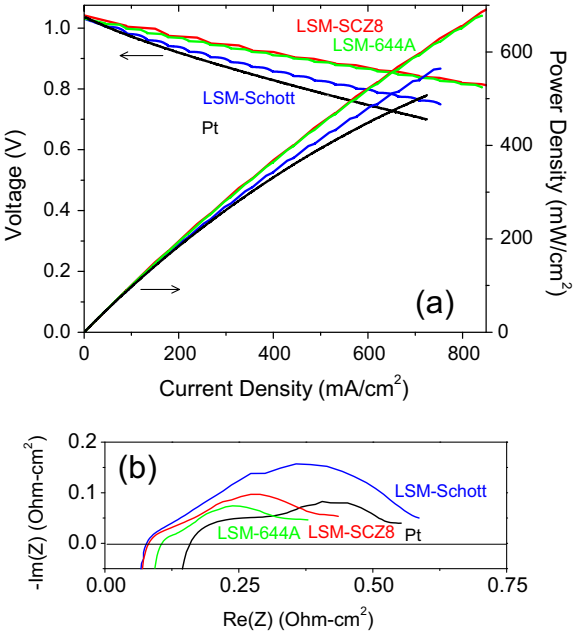

Fig. 5. (a) Polarization and (b) AC impedance data for cells with various CCM types at 800 °C.

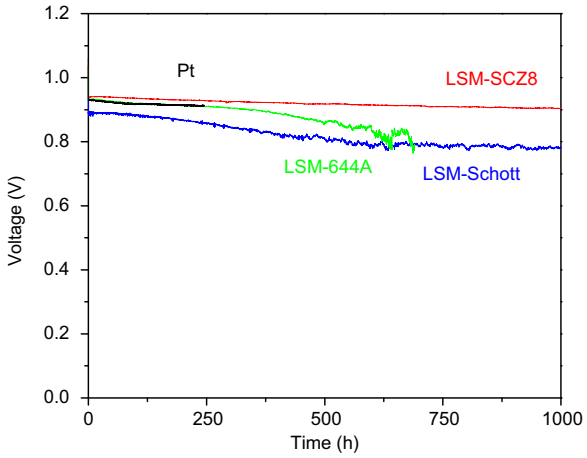

Fig. 6. Long-term operation of cells with various CCM types at 800 °C, 300 mA cm^{-2}.

of SCZ8 to the materials set does not seem to compromise cell performance or stability. Fig. 7(b) shows that the non-ohmic impedance changed minimally after operation. This is consistent with the LSCF cathode remaining unaffected by the presence of SCZ8 in the cell. The ohmic portion increased moderately, presumably due to oxidation of the steel current collecting mesh discussed below.

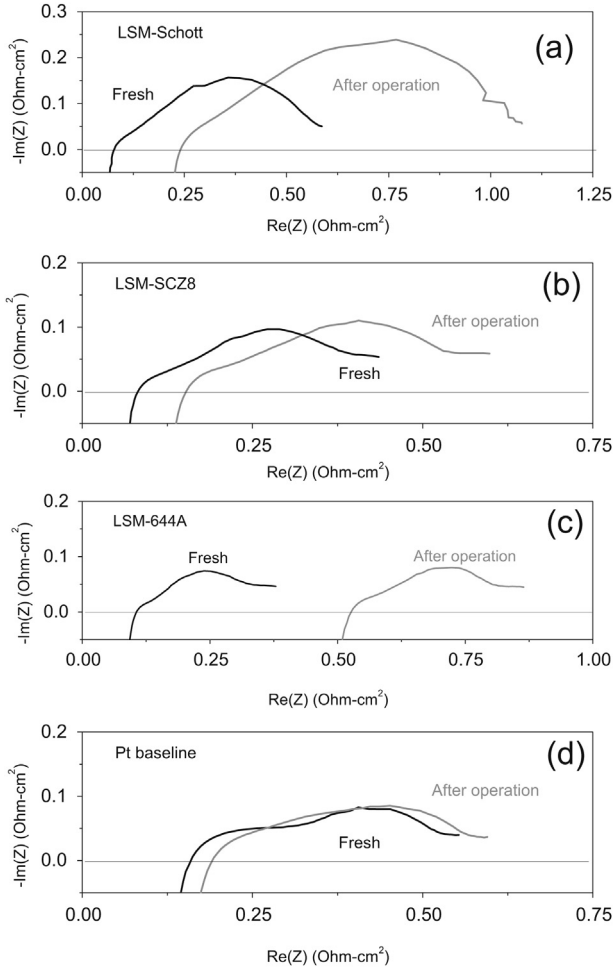

Fig. 7. AC impedance of cells with various CCM types at 800 °C before and after long-term operation.

The cell voltage for the cell with LSM/644A CCM dropped and became erratic toward the end of testing. Formation of a small hole in the seal was observed upon cooling the cell, and the 441 mesh near the hole had oxidized to the point of brittle failure. Burning hydrogen near the seal defect presumably caused local heating and over-oxidation of the mesh. Therefore, we ascribe the unstable operation at the end of testing to seal issues, and believe it to be unrelated to the presence of 644A on the cell. This is consistent with the AC impedance data (Fig. 7(c)), which showed a large increase in ohmic impedance arising from aggressive oxidation of the steel, but minimal change in the non-ohmic electrode polarization arc, consistent with an unaffected LSCF cathode layer.

After operation, the cells were cross sectioned for SEM/EDS analysis. Fig. 8 shows representative images for the cell containing

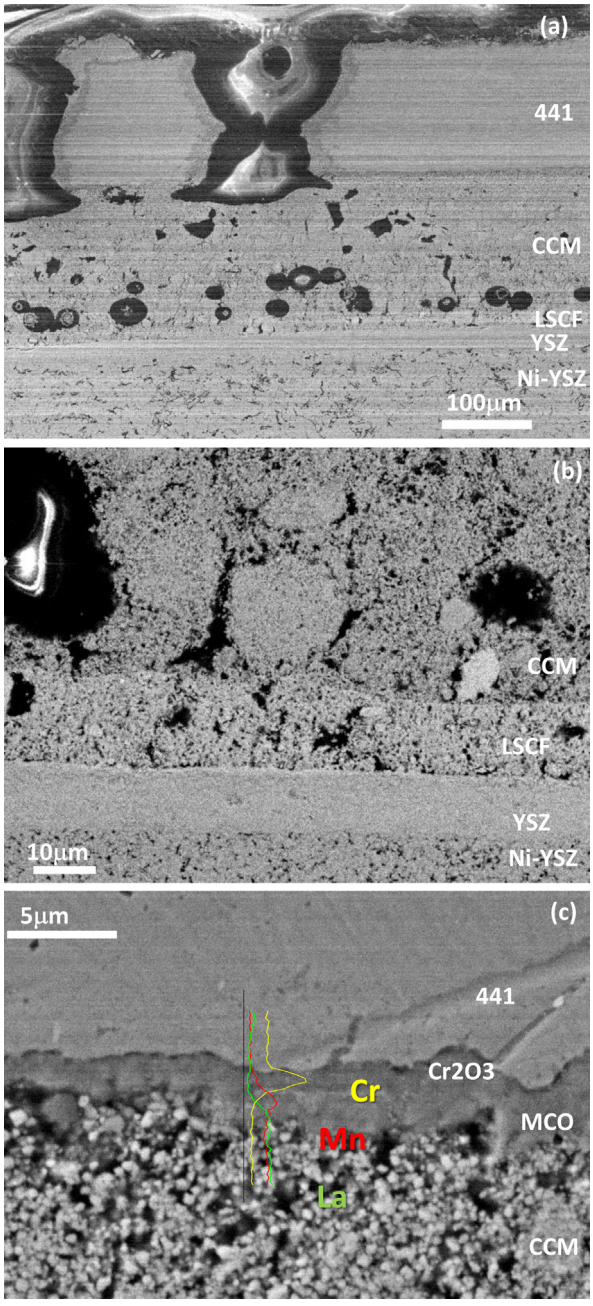

Fig. 8. SEM image of polished cross-section surface of cell and LSM–SCZ8 CCM layer after long-term operation. EDS linescan data for Cr, Mn, and La are overlaid on (c).

LSM–SCZ8 CCM. As seen in Fig. 8(a), the stainless steel mesh, CCM, and cathode catalyst layers are all well adhered. Fig. 8(b) shows a detailed view of the electrochemically active layers. EDS was employed to determine if migration of elements from the CCM additives (glass or inorganic binder) into the LSCF cathode could be identified. Particular attention was paid to the YSZ–LSCF interface (triple phase boundary) and LSCF/CCM interface. For all of the cells, no migration of foreign elements into the LSCF was detected. We therefore conclude that contamination of the electrochemically active sites by the CCM additives did not occur, at least to an extent detectable via EDS analysis. As mentioned above, the ohmic impedance of all the cells increased after operation. Fig. 8(c) shows the steel/CCM interface for the cell with LSM–SCZ8 CCM. A continuous layer of chromia is observed between the steel and MCO coating, roughly 1 μm thick. A chromia layer of similar thickness was observed for all three cells in the active area above the cathode. Therefore, we find that the CCM additives did not have a pronounced effect on oxidation of the steel, for example via degradation of the MCO protective coating.

3.3. Mechanical testing

Previous work with these composite materials suggested that inclusion of a suitable glass or inorganic binder may increase the adhesion of the CCM layer to neighbor materials [3,4]. In this work, we assess the improvement using a more rigorous test and analysis methodology. The CCM and MCO-coated steel interface is typically weaker than the CCM–LSCF interface [3,4]. Therefore, testing focused on the CCM–MCO-coated steel interface. MCO-coated steel coupons were laminated together using the candidate CCM composites. Specimens with pure LSM were also prepared as a baseline.

Fig. 9 shows the load vs. displacement curve obtained for 4-point bending of specimen with LSM–Schott glass CCM. The curve exhibits a linear region up to a load of 4.1 N, when an interfacial crack initiated at the root of the notch. At this point there is a clear change in the slope of the curve and the plateau region of the curve corresponds to the conditions when stable growth of the interfacial crack occurs as the crack propagates outward from the notch. The average value of the plateau load was used to determine the interfacial fracture energy. Post-mortem analysis of this test specimen revealed that the crack propagated preferentially along the interface between the MCO coating and the CCM layer (Fig. 10).

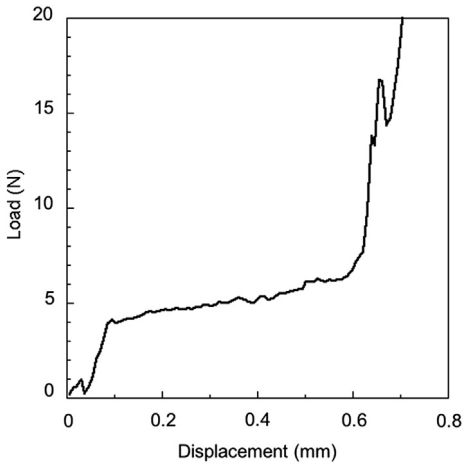

Fig. 9. Load-displacement data for 4-point bending of specimen with LSM–Schott glass CCM.

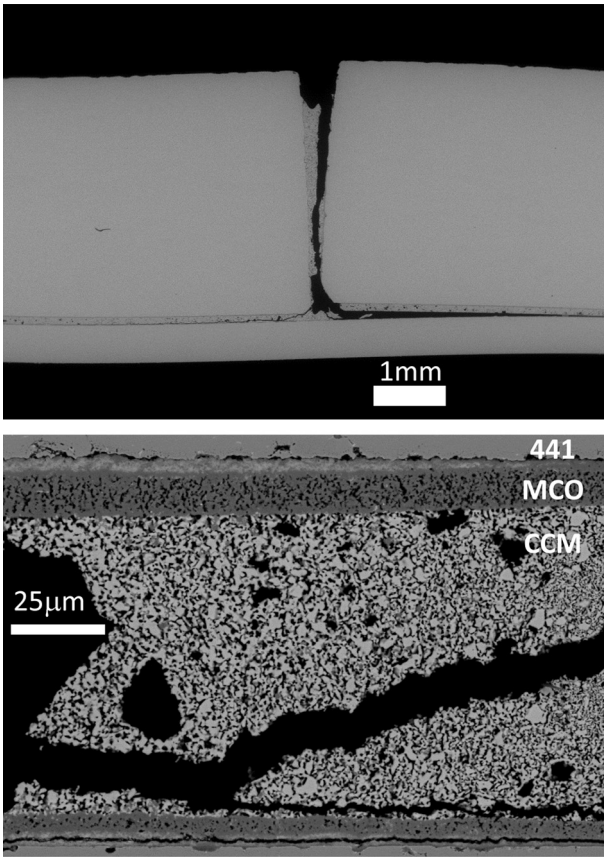

Fig. 10. SEM images of a polished section of specimen with LSM–Schott glass CCM after 4-point bend test.

Although there was also evidence of crack propagation within the CCM layer, it was not possible to determine whether this occurred during the region of stable crack growth or subsequently when the load exceeded the plateau load or during handling for metallographic preparation.

Table 1 compares interfacial fracture toughness for the various CCM types tested. Because there was a relatively wide spread of plateau values recorded, both the average and minimum are reported for each composition. All additives tested provided significant improvement over pure LSM. Even the weakest specimen for each additive was still stronger than pure LSM. It is interesting to note that the largest improvement occurred for addition of Schott glass, which has a softening point much lower than the firing temperature. We surmise that either the glass was incorporated into the LSM matrix during initial sintering (as supported by Ref. [3]), resulting in a much stronger composite, or the presence of residual soft glass over a wider temperature range relieves stress during cooling.

Table 1
Summary of mechanical results for various CCM types.

Interfacial fracture toughness		
Composition	Average (N mm^{-1})	Minimum (N mm^{-1})
LSM	1.7	1.6
LSM + SCZ8	6.8	2.5
LSM + Schott	12.3	4.9
LSM + 644A	5.4	3.9

4. Conclusions

The feasibility of adding inorganic binder or glass to conventional CCM materials in order to improve bonding between SOFC materials has been assessed. Cells with LSM/644A binder, LSM/SCZ8 glass, and LSM/Schott glass composite CCM layers and MCO-coated 441 stainless steel mesh current collectors were operated for up to 1000 h at 800 °C. The cell with LSM/644A showed the best stability of the candidates. None of the CCM candidates led to significant cell damage. Each of the CCM candidates significantly improved interfacial fracture toughness at the CCM/interconnect interface. Addition of Schott glass to the CCM provided the greatest improvement.

Based on these results, we conclude that addition of inorganic binder or glass to the CCM is an effective strategy to improve bonding and mechanical properties of the resulting CCM/binder composite, without sacrificing acceptable electrochemical performance. Addition of SCZ8 glass to LSM was a particularly satisfying example; adhesion strength was significantly improved, while maintaining a high and stable cell performance. All of the candidate compositions studied here performed well enough to warrant further optimization and testing at SOFC operating conditions.

Acknowledgments

This work was supported by the U.S. Department of Energy, National Energy Technology Laboratory and in part by the U.S. Department of Energy under Contract No. DE-AC02-05CH11231. The authors thank Program Manager Joseph Stoffa, and Jeffry Stevenson and Ryan Scott at Pacific Northwest National Laboratory for MCO deposition. The work at ORNL was supported by the U.S. Department of Energy, Office of Fossil Energy, SECA Core Technology Program at Oak Ridge National Laboratory under Contract DE-AC05-00OR22725 with UT-Battelle, LLC.

References

[1] S. Sugita, Y. Yoshida, H. Orui, K. Nozawa, M.U. Arakawa, H. Arai, J. Power Sources 185 (2008) 932–936.
[2] M.C. Tucker, L. Cheng, L.C. DeJonghe, J. Power Sources 196 (2011) 8313–8322.
[3] M.C. Tucker, L. Cheng, L.C. DeJonghe, J. Power Sources 196 (2011) 8435–8443.
[4] M.C. Tucker, L. Cheng, L.C. DeJonghe, J. Power Sources 224 (2013) 174–179.
[5] J. Chen, S.J. Bull, J. Phys. D Appl. Phys. 44 (2011) 034001.
[6] P.G. Charalambides, J. Jund, A.G. Evans, R.M. McMeeking, J. Appl. Mech. 56 (1989) 77–82.
[7] I. Hofinger, M. Oechsner, H.A. Bahr, M.V. Swain, Int. J. Fract. 92 (1998) 213–220.
[8] K. Hilpert, D. Das, M. Miller, D.H. Peck, R. Weib, J. Electrochem. Soc. 143 (1996) 3642–3647.